Design of a narrow span nozzle: a round jet impacting a disk engraved with radial grooves

By SOFIENE OULED TALEB SALAH[1,2,3], NICOLAS DE COCK[1], MATHIEU MASSINON[1], ALEXIS DUCHESNE[3], FREDERIC LEBEAU[1] and STEPHANE DORBOLO[3]

[1]*BioDynE, Gembloux Agro-Bio Tech, University of Liege, Belgium*
[2]*Terra-Agriculture Is life Platform, Gembloux Agro-Bio Tech, University of Liege, Belgium*
[3]*CESAM - GRASP, Institute of Physics, Building B5a, Sart Tilman, University of Liege, Liege, Belgium*
Corresponding Author Email: s.ouled@uliege.be

Abstract

The present work investigates the impact of a turbulent round jet on a motionless disk that is engraved along its circumference by a number *N* of radial grooves. The grooves are used to split the liquid sheet into multiple jets. According to the incoming flow and to the geometry of the grooves, the number of the generated jets *n* correspond to: *2 N* jets, *N** jets (mixed zone), *N* jets and *N/2* jets. The emitted droplets sizes are characterized.

Key words: Groove, jet number, droplet size

Introduction

Plant Protection Product efficiency lies mainly on depositing a maximum portion of the emitted spray on the target and on reducing possible environmental losses as for instance drift issues. Decades of extensive investigation on the spray application field have led to the adoption of drift reduction technologies (DRT) such as shielded sprayers (Ozkan *et al*., 1997) and air assisted sprayers. Other DRT technologies also act on the droplet size distribution by altering the nozzle type and the operating pressure. Shifting the droplet size distribution towards coarse droplets (by increasing the VMD) will reduce the risk of drift because smaller droplets are prone to drift, e.g. anti-drift and air induction nozzle. However, such a practice decreases the treatment efficacy since big droplets (> 350 µm) have the tendency to splash on the target because of their high impact energy (Massinon *et al*., 2015). As a result, in the case for which the secondary droplets will not be intercepted by the neighboring target canopies, they eventually fall to the ground presenting a potential source of contamination. Consequently, an optimal droplet size range as narrow as possible (reduced span) is necessary to minimize retention variability and to reduce drift hazard. In the 90's, rotary atomizers showed that a narrow span spray could be produced by breaking up multiple round jets in the Rayleigh-Plateau regime depending on the jet velocity (Matthews, 1992). The bulkiness of these devices and bad setting use in terms of VMD (i.e. centering the distribution on a VMD which is not favorable to adhesion relative to the surface target) and the direction of the spray (i.e. the horizontal release of droplets attenuates the downward velocity component that is a key component for drift reduction) have dramatically reduced their use. Therefore, the design of a new nozzle with a reduced span remains a challenge for spray practitioners.

Taking inspiration from the rotary atomizers, a round jet impacting vertically a horizontal smooth motionless disk represent the ideal candidate for the massive production of droplets. Such an approach was investigated by Savart who observed many phenomena depending on the ratio (X): the impacted disk diameter D divided by the jet diameter d (X = D/d) (Gordillo *et al.*, 2014). The most relevant case related to our objective corresponds to X ≈ 1 i.e. the round jet impacts the disk center and flows radially to create a liquid film, with a specific thickness, which exceeds the disk edge (thanks to inertia forces) and forms a liquid sheet. Then, the sheet collapses into droplets with various sizes resulting in an extended droplet size distribution (Gordillo *et al.*, 2014). Much focus was made on the radial flow on the disk. The pioneer study was conducted by Watson who showed that the flow behavior could be correctly described by the mean of the boundary-layer theory within a laminar (Watson, 1964; De Cock *et al.*, 2016) and turbulent flow (Watson, 1964). Furthermore, some textured disks were already used in order to study their impacts on the sheet dynamics and hence, the droplet size distribution. For instance, within a laminar flow, the presence of micrometer-sized posts regularly arranged on the disk destabilizes the sheet shape as it adopted polygonal shapes on its rim and generated multiples jets (Dressaire *et al.*, 2013). The spray quality was coarse since jet velocities corresponded to low velocities. In addition, a disk engraved with knife grooves do not destabilize the sheet but it leads to a cardioid shapes formation on its surface (Taylor, 1959).

On this basis, we propose to study the impact of a liquid jet on a motionless disk engraved with deep radial grooves (order of magnitude of the liquid film). The purpose is to simply destabilize the film liquid and create liquid jets of a given size and later droplets with suitable diameters. To obtain enough jets one needs an impact disk of intermediary size (typically X ≈ 10): large enough to engrave a lot of grooves but small enough to reduce the solid friction and also to avoid the hydraulic jump.

Materials and Methods

The nozzle geometry can be simplified as a glass pipe, with an internal diameter d of 3 mm, set perpendicularly on a horizontal disk with a diameter D of 30 mm. The glass pipe generates a cylindrical jet with a mean initial velocity U_0 where $U_0 = 4\,Q\,/\,\pi\,d^2$ (with Q the injected flow rate) and it is characterized by the Reynolds number $Re = U_0\,d\,/\,\vartheta$ (with ϑ is the kinematic viscosity). Re numbers inside the glass pipe are calculated to range between 9000 and 16000 that correspond to a turbulent impact on the disk. The gap between the pipe tip and the plate is 550 µm. The used liquid is tap water ($\sigma = 72$ mN m^{-1}) and it is injected using a gear pump (Ismatec BVP-Z) that delivers a steady liquid flow.

The disk is a plexiglas cylinder cut from a plate with laser cutter. Rectangular grooves are regularly engraved downstream at the edge of the top disk surface and they have a square section of 1 mm side and a length of 5 mm. These grooves are characterized by the inside circular arc d1 (distance) between two successive grooves. This length is given by $d1 = (D\,/\,2 - L)*\,2*\pi/\,N$ where D, L and N represent respectively the disk diameter (m), the groove length (m) and the groove number (Fig. 1).

A high-speed camera is mounted vertically to the disk border to acquire images of liquid sheet and emitted droplets. The images are acquired at a frequency of 2000 Hz and they are analysed with a Particle Tracking Velocimetry Sizing (PTVS) algorithm developed in Matlab (De Cock *et al.*, 2016). In the case of the ungraved disk, droplets are measured 80 mm from the disk edge. The chosen measurement distance takes into account the radius of the sheet radial spreading from the disk (≈ 40 – 50 mm). Then, from the sheet rim to the generated droplets, more distance is required in order to reduce the amount of merged droplet. However, droplet measurements are performed 25 mm from the edge for the engraved disk. Here it is a jet break up regime and the mentioned distance only takes into account the zone where the amount of merged droplets is reduced.

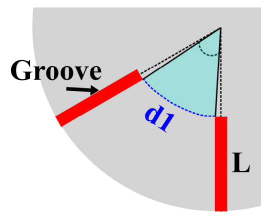

Fig. 1. Representation of the inside circular arc d1 between two neighboring grooves.

Results

Jet regimes and phase diagram

As expected, in the case of a non-textured disk, the impact of the round jet on the disk results in a liquid film that exceeds the disk edge and leads to a sheet. As the impact is turbulent, it triggers the formation of holes (close to the disk edge) in the liquid sheet, which amplify and lead to the disintegration of the liquid sheet (Fig. 2). However, within a laminar regime (low *Re* numbers), the sheet is steady (no holes) and the drops are ejected at the extremities of the cusp indentations located on the sheet rim through a Savart-Plateau-Rayleigh instability (Gordillo *et al*., 2014).

In the case of engraved grooves, we break up the liquid film earlier before reaching the disk edge, what alter the radial sheet dynamics and create several scenarios of liquid jets. Varying *d1* and *Q*, four regimes of jet emissions can be observed and, they are classified by number of emitted jets *n* (Fig. 2). In the case of a stable *n,* two regimes are observed. The first one represents the case where all the liquid is passed through the grooves and hence, one jet per groove is generated and the number of jets *n* is equal to *N*. The second regime is characterized by the emission of main jets from grooves but also by the presence of secondary jets emitted from the gap between two successive grooves. The generated jet number *n* is then equal to *2N*. One can notice that, at the disk exit, the main jets seem more turbulent (noisy) compared to secondary jets. This can be explained by the fact that the main jet follows the shape of the groove section whilst the secondary jet just pass easily with a tangential motion through the gap between two grooves and converges into a jet.

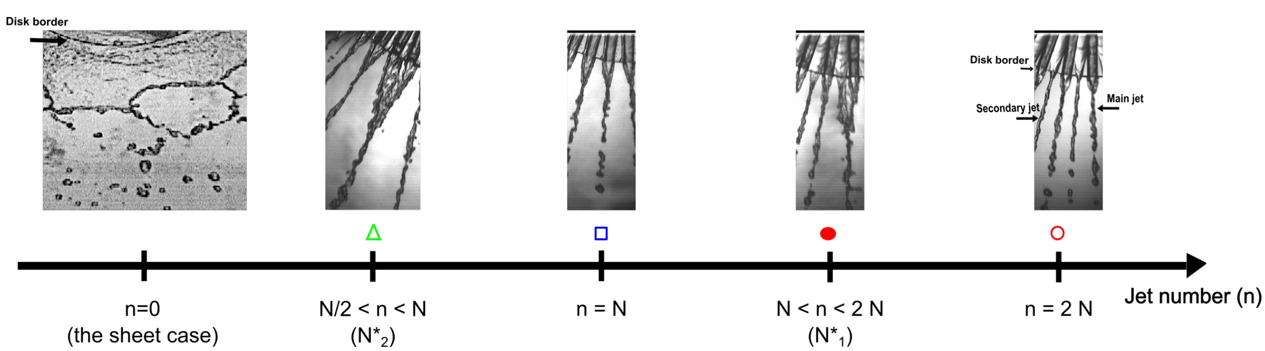

Fig. 2. Representation of the emitted jet numbers (*n*) as a function of engraved grooves.

In the case of a fluctuating n, two regimes are also observed. The first regime represents the case where the secondary jets may locally merge with the main jets and hence, n is between N and $2N$ what lead to the formation of a mixed zone N^*_1. Furthermore, main jets may also coalesce and n is lower than N and greater or equal to $N/2$. Therefore, a second mixed zone N^*_2 is formed. One states that he jet coalescence is elastic in these two cases what explains the fluctuation of n.

For a better understanding of the transition between the observed regimes, a phase diagram is determined by varying Q and $d1$ (Fig. 3). Below a threshold value in $d1$ (= 0.12 mm), only main jets are generated ($n = N$ regime). The internal corners of two successive grooves are too close that the radial liquid is forced to pass through the grooves. In case of high Q, the main jets may merge elastically ($n = N^*_2$ regime). For medium $d1$ (0.12 mm < $d1$ < 0.5 mm), the gap between successive grooves is increased and secondary jets are formed in addition to main jets. Here one observes an elastically coalescence between both kinds of jets for all Q ranges in the $n = N^*_2$ regime. For both high $d1$ values ($d1$> 0.42 mm) and low Q values, main and secondary jets are obtained ($n = 2N$). Then, the secondary jets and main jets may merge elastically with the increase of Q ($n = N^*_1$).

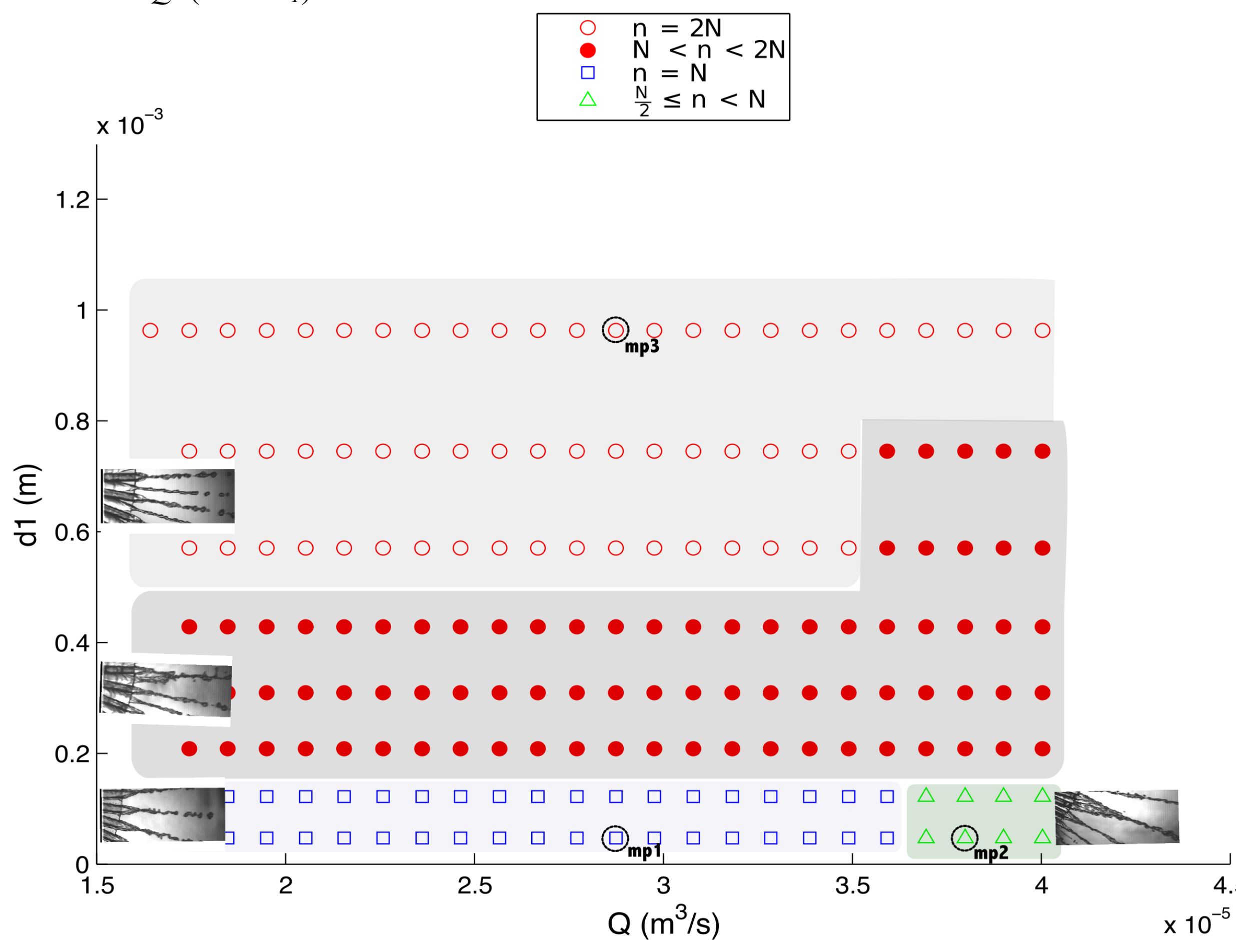

Fig. 3. Representation of different scenarios as a function of $d1$ and Q. Three measurement points of the droplets properties were performed and were designed as $mp1$, $mp2$ and $mp3$.

Characterization of droplet diameters

The emitted droplets from the sheet (case of the reference disk) and jets breakup are addressed. Fig. 4 presents the droplet diameters as a function of their cumulative relative volumes. For the ungraved disk, the measurement is performed at a flow rate Q = 2.8 10^{-5} $m^3.s^1$. Three measurements points are performed in the case of the engraved disk and are designed as *mp1*, *mp2* and *mp3* (drawn in Fig. 3) that correspond respectively to $n = N$ regime, $n = N^*_1$ *regime and* $n = 2\ N$ (*d1* is respectively 0.047 mm, 0.047 mm and 0.963 mm). The two measurements *mp1* and *mp3* are performed at the same Q as used in the case of the ungraved disk. All configurations are compared to a reference standard agricultural flat fan nozzle that is Teejet TP 65 15) within the same spray class (extremely coarse (XC)).
For better readability of curves in Fig. 4, V_{10}, *VMD and* V_{90}, which indicate respectively that 10%, 50% and 90% of the spray volume is composed of drops whose diameters are smaller than this value, are presented in Table 1.

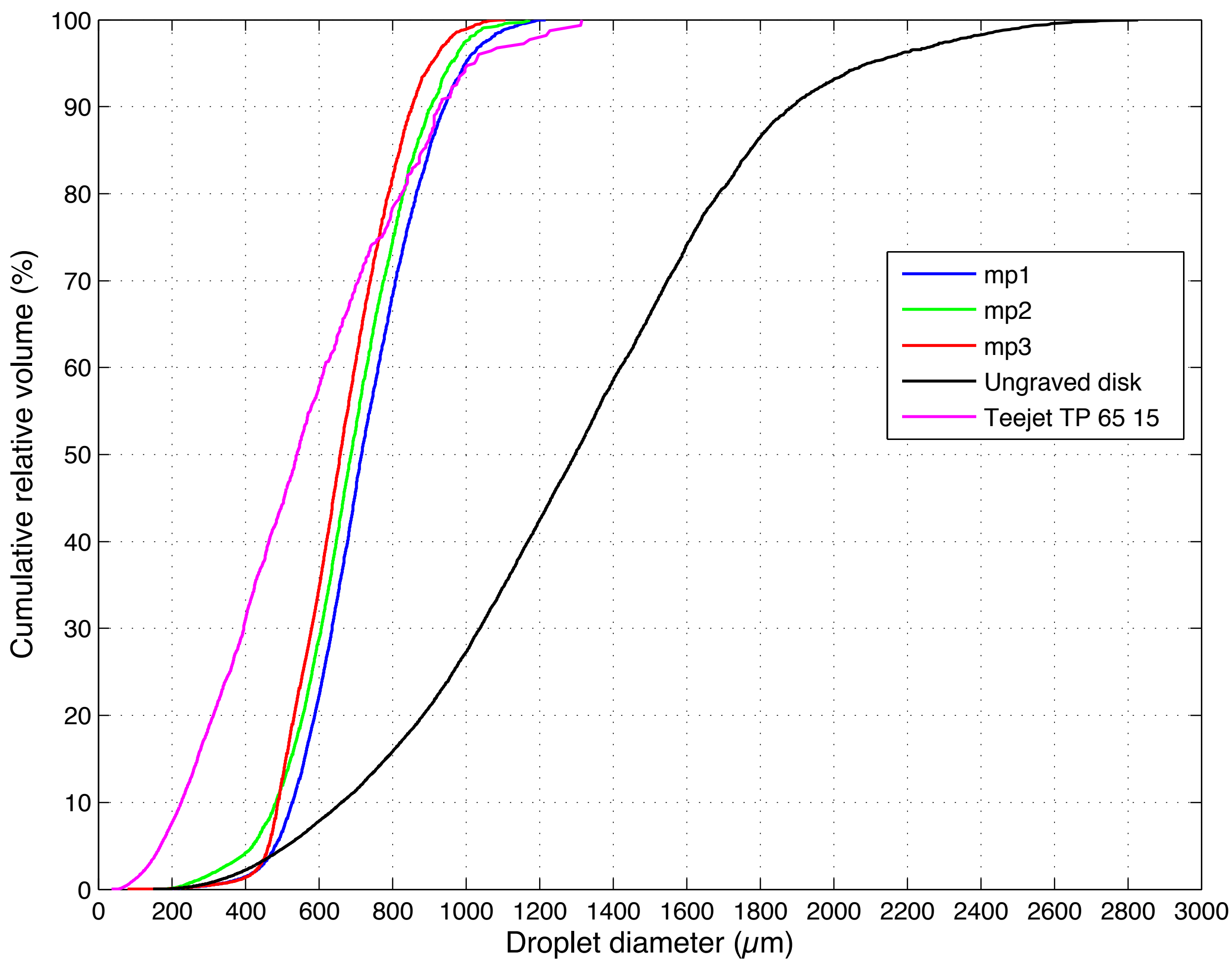

Fig. 4. Representation of droplet diameters as a function of their cumulative relative volumes. Measurements correspond to droplets emitted by the sheet in the case of the ungraved disk and by jets emanating from different scenarios of the liquid sheet on the engraved disk. The measurements points *mp1*, *mp2* and *mp3* correspond respectively to $n = N$, $n = N^*_1$ and $n = 2\ N$ regimes. These cases are compared to a reference standard flat fan nozzle Teejet TP 65 15 within the same spray class (XC).

Table 1. *Characteristics of emitted droplets*

	Q (10^{-5} $m^3.s^{-1}$)	V_{10} (µm)	*VMD* (µm)	V_{90} (µm)	Span	Spray class
Ungraved disk	2.8	662	1297	1886	0.94	XC
mp1	2.8	528	716	941	0.57	XC
mp2	3.8	483	687	905	0.62	XC
mp3	2.8	489	658	853	0.55	XC
Teejet TP 65 15	6.9	225	540	928	1.30	XC

In the case of the ungraved disk, as expected, the droplet size distribution is wide and the quality of the spray is within the extremely coarse (XC) spray class where the VMD is 1297 µm. The extent of the distribution is highlighted by a high span around 0.94 that is close to the span value of hydraulic nozzles (≈ 1). Compared to the reference flat fan nozzle with the same spray class, both cases have the same sheet break up mode but the flat fan nozzle generates finer droplets that is due to the difference of flow conditions, leading also to an extended droplet size distribution. The resulting span is 1.30 and it is in the ranges of the characteristic values of the hydraulic nozzles as indicated above.

Once the disk is ungraved radially with grooves, the sheet break up regime is no longer valid and the jet break up regime occurs. For all the situations involving an engraved disk, i.e. *mp1*, *mp2* and *mp3*, droplet size distributions are tightened and become narrower than the cases of the ungraved disk and the reference nozzle. The reduced droplet size distributions are corroborated by lower span values around 0.5–0.6 that are similar to the span value of rotary atomizers. The spray quality is also finer since the distribution is shifted towards smaller droplets due to the different break up regimes. Hence, the VMD is reduced compared to the ungraved disk but it is larger than the VMD of the nozzle reference due to the difference of flow conditions and the groove geometry.

For the *mp1*, the droplet size distribution is centered on a *VMD* of 716 µm and it represents a span value around 0.57. Furthermore, for mp2 which corresponds to an increase of Q and a transition to $n = N^*_2$ jet zone, the curve keeps the same shape as in *mp1* and the *VMD* is reduced to 687 µm. However, a second droplet population is appeared in contrast with mp1. The unexpected increase of small droplets proportion may be explained by collisions between main jets, which conduct to more small droplets created by other phenomenon than the Plateau-Rayleigh destabilization. Therefore, the droplet size distribution is slightly extended and it is highlighted by span value around 0.62.

For the *mp3* which corresponds to $n = 2\,N$ regime, the curve keeps also the same shape as in *mp1* and the droplet size distribution is centered on a *VMD* of 658 µm. The distribution is more tightened than in *mp1* and it is illustrated by the lowest span value of 0.55. This result may be explained by the fact that the secondary jet emitted between the groove gap is less noisy than the liquid guided by the groove.

Following the Plateau-Rayleigh instability, the droplet diameter is 1.89 times the jet diameter (Dumouchel, 2008) and thus one can expect the *VMD* to be close to 1.89 mm for droplets emitted from a jet issued from a 1 mm side square section groove. This difference is due to that the grooves are not totally filled by the liquid and thus the liquid ejected from the grooves converges in jets smaller than the output grooves sections.

Conclusion

In this paper, the influence of engraved grooves on the sheet dynamics is investigated regarding the droplet production. Firstly, we prove that the groove geometry is able to control the turbulent sheet by splitting the liquid flow in multiple jets before reaching the disk edge. The Phase diagram presented as a function of the parameters *d1* and *Q* highlights the transition between the obtained jet regimes. Smaller liquid jets formed instead of liquid sheet lead to narrower droplet size distributions. The obtained span values are close to those of rotary atomizers. However, much focus is needed to avoid coalescence of jets and to attenuate the roughness of the emitted jets (due to the turbulent regime).

References

De Cock N, Massinon M, Nuyttens D, Dekeyser D, Lebeau F. 2016. Measurements of reference ISO nozzles by high-speed imaging. *Crop Protection* **89**:105–115.

De Cock N, Massinon M, Salah S O T, Mercatoris B, Vetrano M R, Lebeau F. 2016. Dynamics of a thin radial liquid flow. *Fire Safety Journal* **83**:1–6.

Dressaire E, Courbin L, Delancy A, Roper M, Stone H A. 2013. Study of polygonal water bells: inertia dominated thin-film flows over micro-textured surfaces. *Journal of Fluid Mechanics* **721**:46–57.

Dumouchel C. 2008. On the experimental investigation on primary atomization of liquid streams. *Experiments in Fluids* **45**(3):371–422.

Gordillo J M, Lhuissier H, Villermaux E. 2014. On the cusps bordering liquid sheets. *Journal of Fluid Mechanics* **754**:R1.

Massinon M, Dumont B, De Cock N, Ouled Taleb Salah S, Lebeau F. 2015. Study of retention variability on an early growth stage herbaceous plant using a 3D virtual spraying model. *Crop Protection* **78**:63–71.

Matthews G. 1992. *Pesticide application methods*, 2nd Edn. Oxford, UK: Blackwell.

Ozkan H E, Miralles A, Sinfort C, Zhu H, Fox R D. 1997. Shields to reduce spray drift. *Journal of Agricultural Engineering Research* **67**:311–322.

Taylor G. 1959. The Dynamics of Thin Sheets of Fluid, I. Water Bells. *Proceedings of the Royal Society, A* **253**(1274):289– 295.

Watson E. 1964. The radial spread of a liquid jet over a horizontal plane. *Journal of Fluid Mechanics* **20**(03):481–499.